Pulling Monatomic Gold Wires with Single Molecules: An *Ab Initio* Simulation

Daniel Krüger,[1] Harald Fuchs,[1] Roger Rousseau,[2] Dominik Marx,[2] and Michele Parrinello[3]

[1]*Physikalisches Institut, Westfälische Wilhelms-Universität Münster, Wilhelm Klemm-Strasse 10, 48149 Münster, Germany*
[2]*Lehrstuhl für Theoretische Chemie, Ruhr-Universität Bochum, 44780 Bochum, Germany*
[3]*Swiss Center for Scientific Computing/ETH Zurich, Via Cantonale, Galleria 2, 6928 Manno (TI), Switzerland*
(Received 30 April 2002; published 10 October 2002)

Car-Parrinello molecular dynamics simulations demonstrate that pulling a single thiolate molecule anchored on a stepped gold surface does not preferentially break the sulfur-gold chemical bond. Instead, it is found that this process leads to the formation of a monoatomic gold nanowire, followed by breaking a gold-gold bond with a rupture force of about 1.2 nN. The simulations also indicate that previous single-molecule thiolate-gold and gold-gold rupture experiments both probe the same phenomenon, namely, the breaking of a gold-gold bond within a gold nanowire.

With continuing advances in molecular electronics and miniaturization focus is turning to the properties of single-molecule organometallic contacts. One of the most prominent of these systems are thiolates on or between gold surfaces. Single-molecule experiments using a mechanically controllable break junction [1] and atomic force microscope (AFM) [2] gave the first insights into their response to external electric voltage [3] or mechanical stresses. As yet, unrelated findings have been the observation of homonucleus gold nanopoint contacts [4–7] and monoatomic gold nanowires. To relate these findings, a detailed understanding of the interplay of chemical and mechanical properties of such contacts is required. While molecular dynamics simulations based on empirical descriptions of the atomic interactions [8,9] could contribute significantly to our understanding of such observations, approaches that include the electronic structure are mandatory for the more complex organometallic junctions [7,10–19].

In order to cope with this challenge we have employed Car-Parrinello molecular dynamics [20,21] to investigate the rupture process of an ethylthiolate molecule (CH_3-CH_2-S) on gold at room temperature. The calculations were performed with the CPMD code [21,22] using the BP86 functional, Troullier-Martins pseudopotentials for C and S, and a 60 Ry plane wave energy cutoff using the Γ point only. For Au, an 11 electron scalar-relativistic dual-space pseudopotential [23] is employed. The performance of this approach was evaluated in a previous study [24] including several functionals, post-Hartree-Fock methods, and small-core pseudopotentials. The Au(221) surface was selected as an Au(111) vicinal surface. It exhibits both four row Au(111) terraces as well as step edges which are expected to mimic surface heterogeneities and defects as present on real surfaces. The corresponding slab is arranged in four layers of gold atoms where the bottom two layers were fixed at their optimized bulk positions in a triclinic periodic supercell

with lateral lattice vectors of 9.61 and 12.16 Å and up to 27.4 Å normal to the surface. It is well known that small gap and, in particular, metallic systems suffer from undesired heat transfer from the ionic into the fictitious electronic degrees of freedom during finite-temperature Car-Parrinello propagation [21]. This so-called "nonadiabaticity problem" was taken care of by attaching Nosé-Hoover thermostat chains to the electronic degrees of freedom. As an additional test, static pulling simulations were performed by constrained geometry optimization of thiolates adsorbed onto small gold clusters. Here limitations due to finite temperatures, nonadiabaticity, k points, or strain rate are not applicable. Still, these simulations exhibited similar behavior indicating that the results for the much more complex surface slab are *qualitatively* reliable.

In order to study the entire rupture process including the surface our system involved over 650 electrons in a large supercell and required the generation of more than 350 000 configurations (corresponding to about 200 ps of dynamical trajectory). It is clear that fully converged results cannot be expected due to the above approximations that are necessary in order to make such a simulation feasible. However, the Γ-point approximation yields a bulk lattice constant for gold of $a_0 = 4.30$ Å with a bulk modulus of $B = 142$ GPa for a cubic cell of comparable system size. This is close to experiment ($a_0 \approx 4.08$ Å, $B \approx 167$ GPa), and agrees with other calculations that do include k points (for smaller systems) and gradient corrected functionals [13,14,17,18]; note that similar relative errors also apply to Au_2 where k points are no longer an issue [24,25]. The description of the thiolate/gold interactions was carefully assessed based on extensive cluster calculations [24]. A similar accuracy is expected to hold also for the slab calculation since the interactions are fairly local due to the terrace setup with the binding site at the step edge. Based on this analysis, the chosen electronic structure approach in conjunction

with a slab consisting of about 60 Au atoms will produce a sufficiently accurate description of the interactions for our *ab initio* molecular dynamics simulation.

After chemisorption and extensive unconstrained relaxation, the thiolate molecule is found to bind preferentially at the step with an *asymmetric* threefold coordination to gold [Fig. 1(a)] rather than to a site on the terrace, which is in qualitative accordance with experimental observations [26] and recent calculations [14,18]. Most notably, an atomic displacement adjacent to the adsorption site leads to the formation of a vacancy defect at the step edge. This seems reasonable in the light of recent density functional investigations of thiolated gold clusters [24,27] and wires [28] which showed that the chemisorption process leads to a significant perturbation of the underlying gold substrate. This is also consistent with dramatic corrosion processes observed experimentally for alkylthiolates on gold surfaces [29] and the growth of gold atom vacancy islands during the self-assembly process of thiolates on Au(111) [30].

Having prepared a relaxed initial configuration, the terminal carbon $C^\star$ of the thiolate molecule was constrained and successively pulled away from the surface normal to the terrace, i.e., in the $\langle 111 \rangle$ direction, in steps of 0.2 Å at 300 K. For each value of the constraint the force was converged within desired error bars. This discontinuous procedure mimics a very slow process such that "time" is only a meaningful quantity *between* two consecutive steps. The observed reconstructions can be followed with the aid of Figs. 1 and 2 and/or a dynamical animation [31]. The pulling process can be subdivided into four stages; I–III are the initial steps in the formation mechanism of Au nanowires, and IV where wire growth is observed. At a very early stage (stage I, up to ~1.0 Å of elevation of $C^\star$ relative to its initial position) the longest of the 3 S-Au bonds, S-Au3, breaks and the sulfur atom relocates to a more central position above the (111) terrace. The two remaining S-Au contacts, S-Au1 and S-Au2, are relatively stable and a "gold dimer," Au1-

Au2, is subsequently extracted out of the surface (stage II), until it reaches the level of the adjacent upper terrace at ~2.2 Å (stage III). While the dimer raises it remains connected to the step edge up to ~5.0 Å [Fig. 1(b)] at which point the S-Au2 bond breaks (early stage IV), with Au2 relocating to the kink, such that a single gold atom, Au1, now forms a *monoatomic* bridge between the sulfur and the edge of the surface terrace. Upon further pulling (~7.0 Å) Au2 is also extracted from the surface and forms a *diatomic* bridge. When the elongation distance becomes around 10.0 Å, another gold atom follows the same migration path such that finally a *triatomic* gold wire is formed [Fig. 1(c)]. The extracted nanowire adopts a zigzag structure [32] with Au-Au distances in the range of 2.6–2.9 Å. This agrees with the most recent measurement [33] and thus gives no further support to the earlier finding of anomalously large Au-Au spacings [4], see also Ref. [19]. The wire remained stable up to elongations of about 11 Å, beyond which point the Au-Au bond linking the nanowire to the surface breaks. After rupture, a *triangular* Au$_3$ cluster anchored to the thiolate via a single strong S-Au bond, is instantaneously formed due to isomerization [Fig. 1(d)]. It is noted that the finite system size and trajectory length both are factors biasing our simulation towards producing short nanowires.

An essential ingredient in the formation of the wire is the step edge, which actively promotes the elevation of gold atoms out of the (111) terrace. The mean displacement of the gold atoms [Fig. 2(c)] shows the substantial motion within the surface. This is especially true in stage IV, where Au atoms are being extracted from the first surface layer and those from the second move towards the extraction site to replace them. To demonstrate how this occurs, the orthogonal projection of the migration pathways is presented in Fig. 3 which supports the view of the step as a facilitator for the wire formation process. In this representation, stable sites of the crystal surface can be identified visually by dense traces. The most efficient diffusion channel is located between the adsorption site
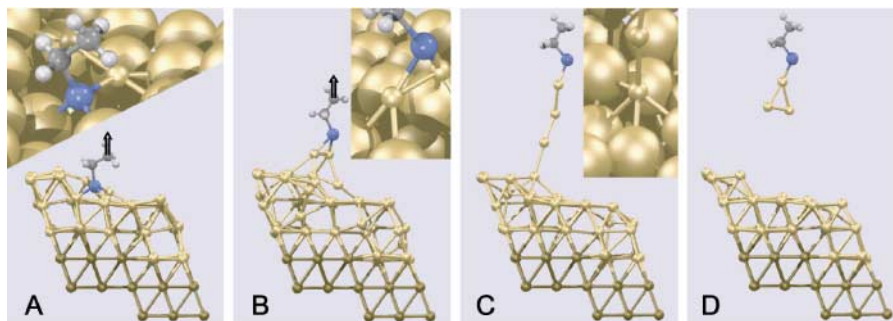
FIG. 1 (color).   Snapshots at different stages of the pulling process [31] at four elevations of the terminal carbon atom $C^\star$ of ethylthiolate relative to its relaxed initial position (a) 0.0 Å, (b) 5.0 Å, (c) 10.6 Å (d) 11.0 Å. For clarity, parts of the adjacent periodic images are displayed together with the simulation cell and the darkened gold atoms were fixed at their optimized bulk positions. The arrows indicate the pulling direction and the insets magnify the alterations of the contact junction close to the surface. There, gold atoms with a coordination number reduced to half their initial value are depicted by small spheres, which visualizes the extraction process from the surface.
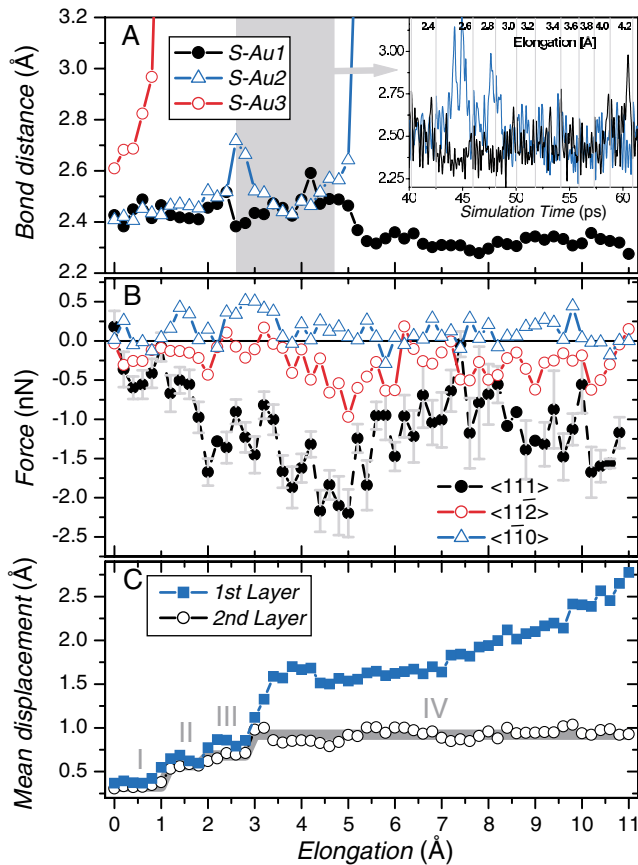
FIG. 2 (color). Observables as a function of the elevation of the terminal carbon atom $C^\star$ of ethylthiolate relative to its relaxed initial position. Panel (a): Sulfur-gold distances of the three closest neighbors to which the sulfur was coordinated initially; see inset in Fig. 1(a). Inset: Time-resolved representation of the dynamics of the bond distances S-Au1 and S-Au2 in the shaded regime. Panel (b): Evolution of the forces in the pulling direction ($\langle 111 \rangle$) and orthogonal to the pulling direction ($\langle 11\bar{2} \rangle$, $\langle 1\bar{1}0 \rangle$); the sign of the pulling force is chosen according to the experimental convention. Panel (c): Mean absolute displacement of the first and the second layer of gold atoms relative to their initial positions. The plateaus I–IV indicate stable stages of the second layer configuration during the pulling process and correspond to the formation of distinct surface species. Stage I, transition from S bound to three Au atoms to two Au atoms forming a "dimeric Au1-Au2 unit." Stage II, dimeric unit within surface terrace and thiolate directly above it. Stage III, dimeric unit above surface terrace with a defect Au atom located directly below the dimer. Stage IV, formation and extraction of a thiolate-terminated gold nanowire.

close to and at the step (Fig. 3). The free energy barrier for the extraction process is furthermore reduced by temporarily created interstitial defects, which are clearly visible close to the extraction locations.

The forces involved in this process—an experimental observable—and their relation to the structural rearrangements are now analyzed in detail. In stage I, the applied force normal to the surface terrace, i.e., the $\langle 111 \rangle$
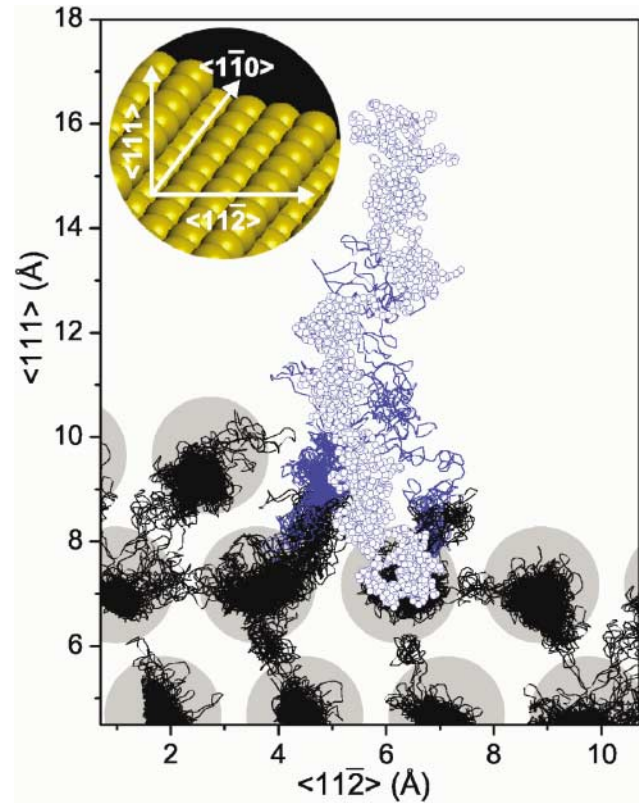
FIG. 3 (color). Orthogonal projection on the $(1\bar{1}0)$ plane, which visualizes the trajectories of the rupture simulation before the wire breaks. The atomic coordinates of the unrelaxed bulk terminated (221) surface without molecule chemisorbed is shown for reasons of clarity (large gray circles). The pathway of those gold atoms that form the wire are marked blue. That of Au1 (which remains directly bound to the sulfur) is highlighted with small blue circles showing its position every 100 configurations. Inset: Crystal lattice vectors of the bulk terminated (221) surface.

component, does not deviate significantly from zero [Fig. 2(b)]. This is concurrent with the change of coordination of sulfur from three to two [Figs. 2(a) and 1(a) → Fig. 1(b)]. The absolute values of the $\langle 11\bar{2} \rangle$ and $\langle 1\bar{1}0 \rangle$ forces orthogonal to the pulling direction are comparatively small during the entire process reflecting the minor lateral motion of the thiolate. While the gold dimer Au1–Au2 is extracted out of the substrate, stages II–IV, the absolute value of the normal force increases steadily until it reaches a peak value of about 2.1 nN at an extension of 4.4–5.0 Å [Fig. 2(b)]. The formation of the *monoatomic* bridge is accompanied by a decrease of the absolute force to almost zero at about 7.4 Å [Fig. 2(b)], where a *diatomic* nanowire standing perpendicular on the surface is formed. Subsequent pulling leads to an increase in magnitude of the normal force to about 1.5 nN at an elongation of 9 Å, followed by yet another decrease foreshadowing the formation of the *triatomic* nanowire. For larger elongation, there is again an increase in the force to 1.5 nN with final rupture occurring at a magnitude of about 1.2 nN.

This overall sawtoothlike behavior, the observation that the rupture force is smaller than the maximum force, and, in particular, also the magnitude of these forces are in astonishing agreement with the combined STM/AFM measurements of a corresponding atomic-sized gold junction [7]. There, the force needed to break one single bond in the gold chain was determined to be 1.5 ± 0.3 nN, while absolute forces clearly exceeding 2.0 nN were obtained at the earlier stages of the elongation process. Interestingly, the quite different thiolate-gold AFM rupture experiments [2] have yielded very similar rupture forces of 1.4 ± 0.3 nN. Thus, our calculations strongly support the idea that the underlying rupture mechanism is identical and that these quite different experiments have probed the same event, namely, the breaking of an Au-Au bond in a gold nanowire.

Given this scenario, the question arises as to why the molecule remains attached in the early stages of the pulling process where actually the largest absolute forces occur. While the loss of the first coordination of the sulfur to the gold (stage I) has no notable impact on the bond length, the loss of the second at 5.2 Å leads to a significant length reduction of the remaining S-Au1 bond as evidenced by the sudden drop in its bond length in Fig. 2(a). Thus, formation of the wirelike configuration *stabilizes* the thiolate-gold contact by strengthening the S-Au1 bond and thereby inhibits the sulfur-gold bond cleavage. This behavior is analogous to the strengthening process found to stabilize monoatomic gold wires in homonuclear gold junctions [7,16].

In conclusion, our rupture simulations of a thiolate on gold display previously unrelated phenomena such as dramatic reconstructions close to chemisorption sites at defects, the formation of monoatomic gold nanowires upon enforced pulling, and the stability of such wires in the presence of thermal fluctuations. Among the key issues for more detailed investigations could be the exploration of different adsorption sites, larger surface slabs, and longer molecular dynamics runs upon the length of the extracted wire. Most importantly, the current study offers a unified and coherent view of experiments that probe various thiolate-gold or gold-gold rupture processes by force spectroscopy and the similar rupture forces involved. Many of the details of the proposed scenario, from chemisorption to cluster formation, are consistent with experiments and/or other calculations that focus on parts of the entire process. Finally, the current study suggests that thiolate molecules on gold surfaces may be *used* as perfectly controllable handles by which monoatomic wires may be drawn and manipulated.

[1] M. A. Reed *et al.*, Science **278**, 252 (1997).
[2] M. Grandbois *et al.*, Science **283**, 1727 (1999).
[3] E. Scheer *et al.*, Nature (London) **394**, 154 (1998).
[4] H. Ohnishi, Y. Kondo, and K. Takayanagi, Nature (London) **395**, 780 (1998).
[5] A. I. Yanson *et al.*, Nature (London) **395**, 783, (1998).
[6] V. Rodrigues and D. Ugarte, Phys. Rev. B **63**, 073405 (2001).
[7] G. Rubio-Bollinger *et al.*, Phys. Rev. Lett. **87**, 026101 (2001).
[8] U. Landman *et al.*, Science **248**, 454 (1990).
[9] M. R. Sørensen, M. Brandbyge, and K.W. Jacobsen, Phys. Rev. B **57**, 3283 (1998).
[10] R. N. Barnett and U. Landman, Nature (London) **387**, 788 (1997).
[11] J. A. Torres *et al.*, Surf.Sci. **426**, L441 (1999).
[12] A. Nakamura *et al.*, Phys. Rev. Lett. **82**, 1538 (1999).
[13] H. Grönbeck, A. Curioni, and W. Andreoni, J. Am. Chem. Soc. **122**, 3839 (2000).
[14] T. Hayashi, Y. Morikawa, and H. Nozoye, J. Chem. Phys. **114**, 7615 (2001).
[15] E. Z. da Silva, A. J. R. da Silva, and A. Fazzio, Phys. Rev. Lett. **87**, 256102 (2001).
[16] S. R. Bahn and K.W. Jacobsen, Phys. Rev. Lett. **87**, 266101 (2001).
[17] M. C. Vargas *et al.*, J. Phys. Chem. B **105**, 9509 (2001).
[18] J. Gottschalck and B. Hammer, J. Chem. Phys. **116**, 784 (2002).
[19] S. B. Legoas *et al.*, Phys. Rev. Lett. **88**, 076105 (2002).
[20] R. Car and M. Parrinello, Phys. Rev. Lett. **55**, 2471 (1985).
[21] D. Marx and J. Hutter, in *Modern Methods and Algorithms of Quantum Chemistry*, edited by J. Grotendorst (NIC, FZ Jülich, 2000), pp. 301–449; see www.theochem.ruhr-uni-bochum.de/go/cprev.html
[22] J. Hutter *et al.*, CPMD Version 3.0, MPI-FKF and IBM.
[23] C. Hartwigsen, S. Goedecker, and J. Hutter. Phys. Rev. B **58**, 3641 (1998).
[24] D. Krüger *et al.*, J. Chem. Phys. **115**, 4776 (2001).
[25] B. A. Hess and U. Kaldor, J. Chem. Phys. **112**, 1809 (2000).
[26] M. M. Walczak *et al.*, J. Electroanal. Chem. **396**, 103 (1995).
[27] I. L. Garzón *et al.*, Phys. Rev. Lett. **85**, 5250 (2000).
[28] H. Häkkinen, R. N. Barnett, and U. Landman, J. Phys. Chem. B **103**, 8814 (1999).
[29] K. Edinger, M. Grunze, and Ch. Wöll, Ber. Bunsen-Ges. Phys. Chem. **101**, 1811 (1997).
[30] G. E. Poirier and E. D. Pylant, Science **272**, 1145 (1996).
[31] See EPAPS Document No. E-PRLTAO-89-019244 for an animation of the entire rupture process. A direct link to this document may be found in the online article's HTML reference section. The document may also be reached via the EPAPS homepage (http://www.aip.org/pubservs/epaps.html) or from ftp.aip.org in the directory /epaps/. See the EPAPS homepage for more information.
[32] D. Sánchez-Portal *et al.*, Phys. Rev. Lett. **83**, 3884 (1999).
[33] Y. Takai *et al.*, Phys. Rev. Lett. **87**, 106105 (2001).